

# 1 **Comparison of lightning activity in the two most active areas** 2 **of the Congo Basin**

3 Jean K. Kigotsi<sup>1,2</sup>, Serge Soula<sup>1</sup>, Jean-François Georgis<sup>1</sup>

4 <sup>1</sup>Laboratoire d'Aérodynamique, Université de Toulouse, CNRS, Toulouse, France

5 <sup>2</sup>Département de Physique, Faculté des Sciences, Université de Kinshasa, République Démocratique du Congo

6 *Correspondence to:* Jean K. Kigotsi (jeankigotsi@gmail.com); Serge Soula  
7 (serge.soula@aero.obs-mip.fr)

8 **Abstract.** A comparison of the lightning activity in the two most active areas (Area\_max for  
9 the main maximum and Area\_sec for the secondary maximum) of the Congo basin is made  
10 with data obtained by the World Wide Lightning Location Network (WWLLN) during 2012  
11 and 2013. Both areas of same size ( $5^\circ \times 5^\circ$ ) exhibit flash counts in a ratio of about 1.32 for  
12 both years and very different distributions of the flash rate density (FRD) with maximums in a  
13 ratio of 1.94 and 2.59 for 2012 and 2013, respectively. The FRD is much more widely  
14 distributed in Area\_sec, which means the whole area contributes more or less equal to the  
15 lightning activity. The diurnal cycle is much more pronounced in Area\_max than in Area\_sec  
16 with a ratio between the maximum and the minimum of 15.4 and 4.7, respectively. However,  
17 the minimum and maximum of the hourly flash rates are observed roughly at the same time in  
18 both areas, between 07:00 and 09:00 UTC and between 16:00 and 17:00 UTC, respectively.  
19 In Area\_sec the proportion of days with low lightning rate (0-1,000 flashes per day) is much  
20 larger (~45% in 2013) compared to Area\_max (~23% in 2013). In Area\_max the proportion  
21 of days with moderate lightning rate (1,001-6,000 flashes per day) is larger (~68.5% in 2013)  
22 compared to Area\_sec (~46% in 2013). The very intense convective events are slightly more  
23 numerous in Area\_sec. In summary, the thunderstorm activity in Area\_sec is more variable at  
24 different scales of time (annually and daily), in intensity and in location. Area\_max combines  
25 two favourable effects for thunderstorm development, the convergence associated with the  
26 African easterly jet of the Southern Hemisphere (AEJ-S) and a geographic effect due to the  
27 orography and the presence of a lake. The location of the strong convection in Area\_sec is  
28 modulated by the distance of westward propagation/regeneration of MCSs in relation with the  
29 phase of Kelvin waves.

## 30 **1 Introduction**

31 According to several studies about the lightning climatology around the Earth, the Congo  
32 basin is considered as the most active region with either a large maximum, or two distinct  
33 ones (Christian et al., 2003; Williams and Satori (2004), Albrecht et al., 2011, 2016, Cecil et  
34 al., 2014, Soula et al., 2016). Actually, the features of the maximum area depend on the  
35 spatial resolution considered in the calculation of the flash rate density (FRD) and the scale  
36 resolution in the graphic representation. Albrecht et al. (2016) performed a very detailed  
37 analysis of FRD thanks to Lightning Imaging Sensor (LIS) data around the Earth, by using  
38 several spatial resolutions. They showed the features of the maxima FRD strongly depend on  
39 the spatial resolution and on the duration of the period considered for the study. Thus, the  
40 location and the value of the first- and second-ranked maxima FRD stabilize when the period  
41 is longer. With the better resolution ( $0.1^\circ$ ) used in Albrecht et al. (2016), the second-ranked  
42 hotspot is always located around [ $28^\circ\text{E}$ ;  $2^\circ\text{S}$ ] from five years of data. Furthermore, they  
43 showed most of the first ten lightning hotspots over the entire African continent, including the  
44 strongest ones, are located in Democratic Republic of Congo (DRC). By considering the maps  
45 of FRD in Albrecht et al. (2016), the existence of two regions of maximum activity in DRC is  
46 displayed but the non linear scale does not allow a quantitative comparison of the maximum  
47 values.

48 Cecil et al. (2014) provided two maps of lightning flash density from the Lightning Imaging  
49 Sensor (LIS) and Optical Transient Detector (OTD) data with different resolution,  $0.5^\circ$  and  
50  $2.5^\circ$  and a non linear scale. With a  $0.5^\circ$  resolution, two maxima are distinguished in the region  
51 of Congo Basin and only one with a  $2.5^\circ$  resolution. Two separated maxima are also visible in  
52 the study by Christian et al. (2003) with a resolution of  $0.5^\circ$  and a non-linear scale of density.  
53 However, in the latter study, neither maximum remain throughout the year in considering the  
54 lightning activity with 3-month seasons. Recently, Soula et al. (2016) showed a very  
55 pronounced maximum in the annual and seasonal lightning flash density in the eastern  
56 Democratic Republic of Congo (DRC) from World Wide Lightning Location Network  
57 (WWLLN) data with a  $0.1^\circ$  resolution and a linear scale. In this study, a secondary maximum  
58 was also highlighted west of the main maximum, especially during the first part of the 9-year  
59 period of study. This secondary maximum was less pronounced and scattered ~~in~~ over a large  
60 area. In this study the region of maximum activity could be analyzed in detail because the  
61 linear scale for flash density was better adapted for large values compared to previous studies.

62 The results of Soula et al. (2016) provided the following characteristics. The main  
63 maximum in lightning flash density is observed every year in one small region of the DRC, at  
64 about 28°E and between 1°S and 2°S. This maximum is embedded within a region of large  
65 values of lightning flash density strongly contrasting with the whole study area. The  
66 geographical extent of this region is approximately 300 km north-south and 200 km east-west.  
67 It is located in the area where many authors identified the maximum of the planetary lightning  
68 activity, as Christian et al. (2003) who falsely attributed it to Rwanda, Cecil et al. (2014) and  
69 Albrecht et al. (2011). The high spatial resolution and the linear scale used in Soula et al.  
70 (2016) allowed a better localization and specification of its shape and amplitude  
71 characteristics. In addition, the maximum number of days with thunderstorms has been found  
72 in the same area (189 days of storms in 2013) as the average number of flashes per day of  
73 storms (approximately 8 flashes per day). Another area of large flash density considered as a  
74 secondary maximum was pointed out in Soula et al. (2016). This area was broader but less  
75 contrasting from year to year during the period of the study. It extends roughly from the  
76 centre of DRC to Congo to the west and to Angola to the south.

77 The goal of this study is to compare the characteristics of lightning activity in the two areas  
78 of maximum activity. The second section describes the data and the methodology used, the  
79 third section presents the results from several comparisons, and the fourth section is devoted  
80 to a discussion.

## 81 **2 Data and methodology**

82 By following the study by Soula et al. (2016), we define two areas of equal area, one for the  
83 main maximum considered as “Area\_max” and the other for the secondary maximum  
84 considered as “Area\_sec”. They are identified by latitude and longitude values in the  
85 following intervals:

86 [25°E; 30°E] and [4°S; 1°N] for Area\_max

87 [18°E; 23°E] and [4°S; 1°N] for Area\_sec

88 We use data from the WWLLN for the present study. The WWLLN ([www.wwlln.net/](http://www.wwlln.net/)) is  
89 a global lightning detection network around the Earth. The electromagnetic radiation emitted  
90 by lightning strokes (from cloud-to-ground and intracloud flashes) at very low frequency  
91 (VLF) and called sferics are detected by the sensors of the WWLLN (Abarca et al., 2011).  
92 These strokes are then localized by using the time of group arrival technique (TOGA)  
93 (Dowden et al., 2002). The stations can be separated by thousands of km because VLF

94 frequencies can propagate within the Earth-Ionosphere wave guide with very little  
95 attenuation. Since its implantation in March 2003, the WWLLN has been improved in terms  
96 of number of stations and development of the processing algorithm (Rodger et al., 2008). In  
97 order to give an idea of the growth of the number of WWLLN stations spread on the planet, it  
98 was 11 in 2003, then 23 in 2005, 30 in 2007 and 67 in 2013, according to the report made by  
99 Rodger et al. (2014). Indeed, the changes in the network during this 9-year period (2003-  
100 2013) can explain the continuous increase of the detection efficiency (DE) observed by Soula  
101 et al. (2016) in the total domain of the study. According to Abarca et al. (2011), DE for CG  
102 flashes is about twice that for IC flashes.

103 We analyze the DE evolution during this period for each area. For this purpose and in the  
104 same way as Soula et al. (2016) for the whole Congo basin area, Figure 1 displays the annual  
105 numbers of lightning flashes detected by WWLLN and LIS in Area\_max and Area\_sec during  
106 the period 2005-2013. In the same graph, the values of the WWLLN DE relative to the LIS  
107 data, are reported for each area. DE is calculated by following the methodology developed by  
108 Soula et al. (2016), i.e. by applying the correction coefficient for the estimation of the number  
109 of the whole lightning flashes LIS could detect with a continuous survey. First, the number of  
110 flashes detected by LIS in each area does not vary much during the period, it is always larger  
111 in Area\_max, its minimum is observed for 2007 in each area and more pronounced for  
112 Area\_sec, and the maximum is observed for 2005 in each area too. Thus, no increase  
113 tendency is observed in each area. Secondly, the number of flashes detected by WWLLN in  
114 each area increases after 2008, especially during the last two years 2012 and 2013. As a  
115 consequence, DE is significantly larger for 2012 and 2013, and reaches 4.96% and 7.50% in  
116 Area\_max, respectively, and 4.24% and 6.11% in Area\_sec. This increase of DE is  
117 completely independent of the number of flashes detected by LIS that is relatively stable  
118 during the last years, which means it is totally related to the WWLLN performance.  
119 According to the DE values, we select the last two years of the period (2012 and 2013) for a  
120 comparison of the characteristics of the lightning activity in Area\_max and Area\_sec.

## 121 **3 Results**

### 122 **3.1 Spatial distribution of the lightning activity**

123 Figure 2a-b shows the annual FRD, in flash km<sup>-2</sup> yr<sup>-1</sup>, calculated with a resolution of 0.05°  
124 from WWLLN data in the large domain of the Congo basin for 2012 and 2013, respectively.  
125 Figure 2c-d shows the number of days of the year with lightning activity in the same domain

126 with the same resolution for 2012 and 2013, respectively. The white frames indicate the two  
127 areas with strong activity (left Area\_sec and right Area\_max). Table 1 displays the flash  
128 count, the maximum FRD for both areas and for each year. Both areas of same size ( $5^\circ \times 5^\circ$ )  
129 exhibit total flash counts in a ratio of about 1.32 for both years, which indicates a stable  
130 situation from one year to the next. On the contrary, the ratio of the maximum FRD is very  
131 different from one year to the next, since it is 1.94 and 2.59 for 2012 and 2013, respectively.  
132 This difference can be easily understood since the maximum value is very localized and can  
133 change substantially from one year to the next, and furthermore the spatial density resolution  
134 used in the study is very high, with a value of  $0.05^\circ$ . The maximum value of the density  
135 depends on the spatial resolution, in the sense that it increases when the resolution becomes  
136 higher. By comparing with the values reported by Soula et al. (2016) at a resolution of  $0.1^\circ$ , it  
137 is clear that the maximum of the annual FRD is larger for  $0.05^\circ$ . Indeed, it is  $12.86 \text{ fl km}^{-2} \text{ yr}^{-1}$   
138 at  $0.1^\circ$  and  $15.33 \text{ fl km}^{-2} \text{ yr}^{-1}$  at  $0.05^\circ$  in 2013, and it is  $8.22 \text{ fl km}^{-2} \text{ yr}^{-1}$  at  $0.1^\circ$  and  $8.62 \text{ fl km}^{-2}$   
139  $\text{yr}^{-1}$  at  $0.05^\circ$  in 2012. On the other hand, the maximum number of stormy days is lower with  
140 the resolution of  $0.05^\circ$ , from 189 to 125 days for 2013 and from 167 to 99 days for 2012. This  
141 observation is consistent since a day is stormy when at least one flash is detected in the pixel.

142 The difference between the distributions in the two areas clearly appears regarding both  
143 lightning FRD and number of days of the year with lightning activity in Figure 2. Indeed, the  
144 highest values of both parameters are located in the same region of the  $5^\circ \times 5^\circ$  frame for  
145 Area\_max while they are much more scattered in the frame for Area\_sec. The difference  
146 between both areas is stronger for FRD compared to the number of days with thunderstorms,  
147 which means that the number of flashes per stormy day is larger for Area\_max. It means that  
148 the storms in Area\_max are more active and/or more stationary, and/or more numerous (Soula  
149 et al., 2016). The differences observed in the maximum values and the distributions of the  
150 lightning FRD indicate specific conditions for the thunderstorm development in Area\_max.  
151 These conditions are the presence of a mountain range that exceeds 3000 meters ( $28.75^\circ\text{E}$ ;  
152  $1.5\text{-}2.2^\circ\text{S}$ ), on the west side of which the FRD increases markedly, and the presence of the  
153 lake Kivu ( $29.2^\circ\text{E}$ ;  $1.9^\circ\text{S}$ ) above which the FRD increases (Soula et al., 2016). No specific  
154 shape of the FRD or stormy day is visible in Area\_sec.

### 155 **3.2 Daily cycle**

156 Figure 3 shows the daily cycle of the flashes detected by the WWLLN in Area\_max and  
157 Area\_sec, for 2012 and 2013. The time is indicated in UTC, which is two hours late compared  
158 to Local Time ( $\text{LT} = \text{UTC} + 2$ ). These flash counts are calculated over one hour and averaged

159 over all days of the year. The time scale of the graph is made so that the flashes are associated  
160 with the beginning of the 1-hour period of calculation. Both areas exhibit the same type of  
161 diurnal lightning activity with a large proportion of flashes during the afternoon and whatever  
162 the year. The minimum and maximum numbers of flashes are observed roughly at the same  
163 time in both areas. The minimum is observed in the morning between 08:00 and 09:00 UTC  
164 for Area\_max and between 07:00 and 08:00 UTC for Area\_sec, for both years. The maximum  
165 is observed in the afternoon, between 16:00 and 17:00 UTC for Area\_max and for both years  
166 and for Area\_sec in 2013, and between 17:00 and 19:00 UTC for Area\_sec in 2012. The  
167 contrast in flash counts between the morning minimum and the afternoon maximum is  
168 stronger for Area\_max (ratio of 14.5 and 15.4, for 2012 and 2013, respectively) than for  
169 Area\_sec (ratio of 6.2 and 4.7, for 2012 and 2013, respectively). It means the diurnal cycle is  
170 much more pronounced in Area\_max. Consequently, while the lightning flash rate is larger in  
171 Area\_max for the main part of the day, it is lower during a short interval between 06:00 and  
172 10:00 UTC corresponding to the minimum activity in both areas.

### 173 **3.3 Day-to-day variability**

174 We compare the lightning activity in both areas in terms of daily distribution of flashes  
175 detected during one year. The years of reference are 2012 and 2013 with a total of 366 and  
176 362 days, respectively, available in the database. The flash count is performed day by day in  
177 each area and then the days are classified by range of flash numbers. Thus, Table 2 displays  
178 the result of the classification for each area and each year, over 12 classes of flash number.  
179 This result is expressed in terms of number of days for each area and year, and in proportion  
180 (%) of the total number of days for the year in each area. The incrementing of each class is  
181 done on 1,000 flashes, except for the class CL1 that is on 900 flashes from 101 to 1,000  
182 flashes. The first class CL0 corresponds to 0-100 flashes to distinguish the days with a very  
183 low number of flashes. The last class CL11 groups the days with more than 10,000 flashes. To  
184 make easier the interpretation of the results, they are also plotted in Figure 3.

185 The distribution is similar for both years, (a) for 2012 and (b) for 2013. The number of days in  
186 CL0 is much larger for Area\_sec than for Area\_max (59 and 7, respectively, in 2012, 43 and 4  
187 in 2013), as indicated in Table 2. For CL1 corresponding to the flash numbers 101-1,000, the  
188 number of days is also larger for Area\_sec, slightly in 2012 with 130 and 121 days,  
189 respectively, markedly in 2013 with 121 and 80 days, respectively. On the contrary, the  
190 number of days for classes corresponding to intermediate flash numbers (CL2 to CL4 in 2012,

191 CL2 to CL6 in 2013) is significantly larger for Area\_max, for both the cumulative number of  
192 days (202 against 144 in 2012 and 248 against 168 in 2013) and for each class considered  
193 separately. For the classes with a very high activity (CL5 to CL11 and CL7 to CL11, in 2012  
194 and 2013, respectively) the total number of days is small and not very different in both areas  
195 (36 and 30 in 2012, 20 and 30 in 2013, for Area\_max and Area\_sec, respectively).

196 From 2012 to 2013, for both areas, the proportion of the number of day decreases in the first  
197 three classes (CL0-CL2) and for the cumulative value it is ~62% in 2012 and ~45% in 2013  
198 for Area\_max, and ~70% in 2012 and ~61% in 2013 for Area\_sec. It is almost equal in CL3:  
199 ~20% in 2012 and ~19% in 2013 for Area\_max, and ~14% in 2012 and ~14% in 2013 for  
200 Area\_sec. It increases almost in all classes after CL3 and for cumulative value it is ~18% in  
201 2012 and ~36% in 2013 for Area\_max, and ~16% in 2012 and ~25% in 2013 for Area\_sec.

### 202 **3.5 Correlation between daily lightning activities**

203 Now we consider the lightning activity for a comparison day by day of both areas to perform  
204 a quantitative correlation. The goal is to evaluate if both areas are simultaneously concerned  
205 by the storm activity or if they are with a shifted time. In order to illustrate the result about  
206 this correlation between lightning activity in Area\_max and Area\_sec, we display the graph of  
207 correlation between the daily lightning flash amounts for both areas and in 2013. These daily  
208 counts are calculated in two ways, first by considering the calendar day (00h00 – 24h00 UT)  
209 and then according the daily cycle of lightning activity between two minimums (06h00 –  
210 06h00 UT, see Figure 2). Figure 5 shows the result of this correlation study: (a) for the  
211 calendar days and (b) for the lightning cycle days.

212 In the first case the correlation coefficient  $R^2$  is ~0.118 and in the second case it is ~0.064.  
213 Thus, the correlation is weak but positive, that is to say the tendency is that when the daily  
214 flash number increases for one area it also increases for the other. At first glance, both  
215 distributions are similar. They reflect the trend highlighted by Figure 4 insofar as the low  
216 values ( $\leq 1000$  flashes per day) are more numerous in Area\_sec. Inversely, the intermediate  
217 values (between 1,001 and 5,000 flashes per day) are more numerous in Area\_max with 230  
218 days in 2013, against 156 days for Area\_sec. For the values exceeding 10,000 flashes per day,  
219 there are 7 days for Area\_max and 5 days for Area\_sec in 2013 (Figure 5a). In Figure 5b,  
220 these values are 6 and 8, respectively, which means there are more days with a large number  
221 of lightning flashes in Area\_sec, by considering the daily cycle of the lightning activity. This  
222 observation is consistent with the fact that the lightning activity is more widely distributed

223 during the day in Area\_sec as indicated in Figure 3. This may be due to the contribution of  
224 nocturnal lightning by mesoscale convective systems (MCSs) or isolated storms that develop  
225 later in the afternoon if compared to Area\_max. Indeed, the work by Albrecht et al. (2016)  
226 shows in their Figure 3 that during the night, the hotspots located in Area\_sec (i.e, 6th and 7th  
227 Africa's hotspots) exhibit a larger contribution to the daily lightning activity. Thus, by  
228 considering the day according the lightning activity (06h00-06h00), the episodes of strong  
229 lightning activity in this area are more likely to be counted in full.

### 230 **3.6 Month-to-month variability**

231 Figure 6a-b shows the monthly proportion of flashes detected in Area\_max and Area\_sec  
232 during 2012 and 2013. The minimum proportion is found in August and in Area\_sec (between  
233 3 % and 4 %) for both years. The maximum proportion is also found in Area\_sec in May for  
234 2012 (about 14%) and in December (about 14%) for 2013. These two characteristics show  
235 that the variability is always stronger in Area\_sec than in Area\_max although the distribution  
236 is different from 2012 to 2013 for both areas. For example, in April it is 6.1% and 11.3% for  
237 Area\_max, 5.7% and 9.4% for Area\_sec, in 2012 and 2013, respectively. Inversely in May,  
238 the proportion of each area is much lower in 2013 compared to 2012 (4.7% and 8.1% for  
239 Area\_max, 7.9% and 13.9% for Area\_sec). For a given month, the respective proportions for  
240 Area\_max and Area\_sec remain in the same order, except for the first three months of the  
241 year.

242 Figure 6c shows the 3-month proportion over a longer period including data from  
243 2011. The 3-month periods are chosen according to Christian et al. (2003), Jackson et al.  
244 (2009), and Soula et al. (2016). Thus, the months of June, July and August are grouped in  
245 JJA, September, October and November in SON, December, January and February in DJF,  
246 and March, April and May in MAM. The annual variability at this 3-month scale is more  
247 visible and constant from one year to the next. Indeed, for both areas, the minimum is always  
248 in JJA with a constant decrease during the preceding 3-month periods. For the maximum, it  
249 seems SON is more favourable to Area\_max while DJF is for Area\_sec.

## 250 **4 Discussion**

251 Albrecht et al. (2016) studied the lightning hotspots over the Earth, based on satellite optical  
252 observations of lightning. They consider that a hotspot is a region 100-km in radius around a



253 maximum of FRD. They found that six out of the ten most active spots over the whole  
254 African continent, including the three strongest ones, are located in an area corresponding to  
255 Area\_max while only two are located in an area corresponding to Area\_sec. Our results  
256 confirm the predominance of the larger FRD in Area\_max.

257 The characteristics of the diurnal cycle observed in Area\_max and Area\_sec is consistent  
258 with Laing et al. (2011). These authors analyzed the cycle of the deep convection over a large  
259 area of tropical Africa including both areas of our study and during 2000-2003. For two 1-  
260 hour intervals (14:00-15:00 UTC and 17:00-18:00 UTC) besides eight considered in their  
261 study, they found the location of a sharp maximum of the average hourly frequency of coldest  
262 clouds in eastern DRC close to Area\_max. The intervals 15:00-16:00 and 16:00-17:00 UTC  
263 were not plotted in their graphs. They noted this maximum for the two months April and  
264 October analyzed in the study. They also showed that the thunderstorm activity is minimum in  
265 the part of DRC that corresponds to both areas of our study during the time interval 05:00-  
266 06:00 UTC in April and during 08:00-09:00 UTC in October (06:00 and 07:00 UTC were not  
267 plotted). The present observations about minimum and maximum lightning activities  
268 displayed in Figure 2 are consistent with those by Laing et al. (2011). Indeed, the maximum  
269 of the activity is invariably between 16:00 and 17:00 UTC for Area\_max, and in a larger  
270 temporal window for Area\_sec (~17:00-19:00 UTC in 2012 and 16:00-17:00 UTC in 2013).  
271 The maximum storm activity is therefore more variable in time for Area\_sec. The minimum is  
272 invariably between 07:00 and 08:00 UTC for Area\_sec, between 08:00 and 09:00 UTC for  
273 Area\_max. In Albrecht et al. (2016) for the study of lightning hotspots, the daily cycles are  
274 considered for several hotspots located in our areas. They found a daily cycle more pronounced  
275 for the hotspots included in Area\_max compared to the hotspots included in Area\_sec, which  
276 is consistent with the present study.

277 The comparison of the monthly activity in Area\_max and Area\_sec in 2012 and 2013  
278 suggests that the seasonal contrast is stronger in Area\_sec where the maximum monthly  
279 amounts are observed in May and December respectively, and the minimum in August for the  
280 two years. At the seasonal scale, the monthly activity is cumulated over three months  
281 following the average monthly activity found in Soula et al. (2016) for the whole Congo  
282 basin. The inter-annual variability is well visible and reproduced from one year to the next.  
283 Even in these three years the minimum proportion is always in August and in Area\_sec (about  
284 3 to 4%). The maximum proportion is also in Area\_sec but on different months (from 14 to  
285 16%). So the seasonal contrast is much stronger in Area\_sec than in Area\_max. This result,

286 due to the migration of the Intertropical Convergence Zone (ITCZ), is consistent with the  
287 contrast of the seasonal variation in lightning activity found in Soula et al. (2016). Area\_max  
288 is less impacted by the migration of the ITCZ because the triggering of thunderstorms in this  
289 area has a very local origin.

290 The positive correlation observed between the daily activities of the two areas means there  
291 may be an influence between them or a common cause to explain the storm activity. However,  
292 the low value of the correlation coefficient indicates the activities can be different on the  
293 quantitative aspect. Figure 7 displays the daily density of lightning flashes detected by  
294 WWLLN on 25<sup>th</sup> of December 2013 in Area\_sec (a) and in Area\_max (b). This day is  
295 considered because the activity is strong in both areas with 18107 and 10257 flashes detected  
296 in Area\_sec and Area\_max, respectively. Firstly, this distribution shows the lightning density  
297 is high (scale in fl km<sup>-2</sup> day<sup>-1</sup>) in local spots that correspond to convective cores of  
298 thunderstorms. In other words, for a given day, the lightning activity can be strong in a  
299 restricted area and weak around in term of flash number. This characteristic of the storm  
300 activity is well known and pointed out by many works (Carey et al., 2005; Soula et al., 2014).  
301 Secondly, the lightning spots seem east-west elongated in majority, which could indicate a  
302 propagation of the storms within this direction. Thus, the strong activity of a given storm is  
303 probably limited over the time. However, the correlation between both areas probably exists  
304 because of the eastward propagation of conditions favourable to the development of  
305 thunderstorms, as instability of the atmosphere. Indeed, Laing et al. (2011) showed  
306 convection over equatorial Africa can be modulated by different conditions at synoptic scale  
307 for local occurrence or propagation of mesoscale convective systems. They especially  
308 mentioned the eastward-moving equatorially trapped Kelvin waves, the south-westerly  
309 monsoonal flow and the midlevel easterly jets. It is therefore consistent to obtain a low  
310 correlation between our two areas characterized by a strong annual storm activity.  
311 Furthermore, the correlation study is done at the scale of the day and as most thunderstorms  
312 develop at the end of the day, storm activity can occur during the following day in Area\_sec  
313 that is several hundred kilometres to the West.

314 The distribution of storms in the Congo Basin mainly results from four contributions,  
315 namely: development, propagation, merging and regeneration of thunderstorms. As  
316 thunderstorms can develop everywhere in the Congo basin, they can naturally form in both  
317 Area\_max and Area\_sec. However, the great lakes and numerous mountains of Rift valley  
318 close to Area\_max offer most favourable conditions for development and enhancement of

319 thunderstorms. The most intense storms, at planetary scale, are found in the Congo Basin  
320 (Zipser et al., 2006). Area\_max is probably the most active region in the world in terms of  
321 thunderstorms since the number of days of the year with thunderstorm activity is found to be  
322 maximum there (Figure 1c-d) and the density of lightning is large over this extended area  
323 (Soula et al., 2016). On the other hand, according to previous studies, Equatorial Africa  
324 thunderstorms spread from the east to the western Congo basin (Laing et al., 2011; Nguyen  
325 and Duvel, 2008; Laing and Fritsch, 1993). Then thunderstorms may propagate from  
326 Area\_max to Area\_sec but different processes as merging and regeneration may affect their  
327 intensity and induce different characteristics in these areas. Several studies have shown that  
328 heterogeneity of soil moisture or vegetation play a role in thunderstorms triggering (Taylor et  
329 al., 2011; Garcia-Carreras et al., 2010). Furthermore, the modelling results of the Global Land  
330 Atmosphere Coupling Experiment (GLACE) classified Equatorial Africa, including  
331 Area\_max and Area\_sec, among the regions of strong coupling between the atmosphere and  
332 the soil moisture (Koster et al., 2004). Thus, differences of soil moisture and/or vegetable  
333 cover between Area\_max and Area\_sec may contribute to the differences between lightning  
334 activities of the two areas.

335 Farnsworth et al. (2011) pointed out that the MCSs constitute the fundamental unit of  
336 vertical energy transport in Central Africa. In other words, convection in this region generally  
337 leads to the formation of MCSs. This observation is consistent with the results of Liu and  
338 Zipser (2005) and Zipser et al. (2006) (on deep convection in the Congo basin). They showed  
339 convection in the Congo basin frequently overshoots the tropopause. The climatology of  
340 MCSs in Equatorial Africa, including the whole Congo basin, was presented in Jackson et al.  
341 (2009). From a five-year series of data, these authors have shown that the zone on horseback  
342 at the equator between 5°S and 5°N and extending from the Atlantic coast to the west side of  
343 the high mountains of the Rift Valley is the most active in terms of storm activity because it  
344 includes two of four maxima in the number of MCSs that they have identified. In our study,  
345 Area\_max and Area\_sec coincide with the region where Jackson et al. (2009) found the main  
346 number maximum of MCS. Actually, in Jackson et al., two cores appeared in the structure of  
347 this main maximum, one that corresponds to Area\_sec with a less pronounced maximum of  
348 number of MCS and a larger number of lightning flashes per MCS. The second core in  
349 Jackson et al. corresponds to Area\_max with a more pronounced maximum. They explain the  
350 origin of the large number of MCS in this large area by a maximum of midtropospheric  
351 convergence on the west side of the African easterly jet of the Southern Hemisphere (AEJ-S).

352 They observe this condition more pronounced in SON season compared to MAM in the same  
353 way that we observe also more flashes according to Figure 6c. Indeed, according to Mohr and  
354 Thorncroft (2006) and Laing et al. (2008), the vertical shear related to the African easterly jet  
355 (AEJ) influences the location of intense convective systems. Furthermore, mountain ranges  
356 help to initiate long-lived MCSs (Laing et al., 2008; 2011). According to these authors, in all  
357 the regions the convection initiates over the elevated terrain and then propagates in conditions  
358 of moderate vertical shear to develop into mesoscale systems. On the other hand and  
359 according to several authors, the propagation of convection in Equatorial Africa is modulated  
360 by convectively coupled, equatorial Kelvin waves (Laing et al., 2011). During the active  
361 phase of these eastward-propagating large-scale waves, MCSs are larger and more intense.  
362 These convection systems occur farther east from day to day, and propagate westward within  
363 the Kelvin wave envelope. During the dry phase of the Kelvin waves an upper-level  
364 convergence is produced, which eliminates the deep convection and the westward  
365 propagation. Thus, the region corresponding to Area\_max seems to have a stronger maximum  
366 of MCS number, as we find a larger FRD. Area\_max combines two conditions favourable for  
367 thunderstorm activity, the convergence evoked by Jackson et al. (2009) for the large region  
368 and a local orographic effect that reinforces the effect of the first one. Area\_sec seems to take  
369 advantage of the westward propagation/regeneration of MCS, at a distance from the initial  
370 occurrence that depends on the phase of the Kelvin waves, which explains the widespread  
371 large values of FRD observed within this area.

372 The presence of mountains or elevated terrain is always a determining factor in the  
373 mechanism of thunderstorm. For example at a very local scale, Munoz et al. (2016) explain  
374 the role of the topography combined with Nocturnal Low Level Jet in the largest FRD in the  
375 world observed in the region of the lake Maracaibo, Venezuela. At a more global scale,  
376 William and Satori (2004) compared the lightning and rainfall activities in both Amazon and  
377 Congo basins and interpret the greatest FRD observed in Congo basin in terms of features  
378 more continental (drier and warmer) and a larger elevation.

379 According to Zipser et al. (2006) the proportion of intense convective events is larger in the  
380 region corresponding to Area\_sec compared to that corresponding to Area\_max (see their  
381 figure 3). This result is consistent with the present figure 5 concerning the distribution of the  
382 daily flash number in each area, especially the graph (b) where the flash counts are made from  
383 06:00 to 06:00 UTC. Furthermore, the DE is a little lower in Area\_sec compared to  
384 Area\_max, according to the results displayed in Figure 1. Thus, Area\_sec is concerned by a

385 more irregular thunderstorm activity, with both the least active days and the most active days.  
386 It is well illustrated with the example in Figure 7, displaying the daily lightning activity for  
387 the most active day in Area\_sec (see Figure 5a). Indeed, the FRD for the day is more scattered  
388 in the whole area for Area\_sec. The distribution of thunderstorm activity is substantially  
389 different in each area, concentrated with a very marked daily cycle in Area\_max, and  
390 scattered with a daily cycle much less pronounced.

## 391 **5 Conclusion**

392 The spatial and temporal characteristics of the lightning activity are analysed in two areas of  
393 the Congo basin, Area\_max with the strongest thunderstorm activity and Area\_sec with a  
394 secondary maximum. First, the lightning flashes are much more concentrated in the same part  
395 of Area\_max for both years, while they are widespread in Area\_sec. Secondly, the frequency  
396 of days with low activity is larger in Area\_sec and the frequency of days with high activity is  
397 larger in Area\_max. However, the frequency of days with very high activity is similar in both  
398 areas and even the largest daily flash numbers are detected in Area\_sec. Thirdly, a stronger  
399 contrast between the maximum and the minimum in the daily cycle is observed in Area\_max  
400 with a ratio of about 15.4 while it is only 4.7 for Area\_sec. In conclusion, the thunderstorm  
401 activity is more variable in Area\_sec, in terms of location, daytime of occurrence, seasonal  
402 distribution and intensity in terms of number of flashes. These differences are consistent  
403 because Area\_max combines two favourable effects for thunderstorm development, the  
404 convergence associated with the AEJ-S, especially during SON and DJF, and a geographic  
405 effect due to the orography and the presence of a lake. The location of the strong convection  
406 in Area\_sec is widespread, according to the distance and direction of  
407 propagation/regeneration of MCSs that initiate farther eastern, especially in relation with the  
408 phase of Kelvin waves.

## 409 **Acknowledgments**

410 The authors thank the World Wide Lightning Location Network (<http://wwlln.net/>) and  
411 Christelle Barthe from University of la Réunion (France) for providing the lightning location  
412 data used in this study. JK is grateful to the French “Ministère des Affaires Etrangères”, to the  
413 French Embassy in DRC, especially Patrick Demougin, for supporting his stay in France and  
414 “Groupe International de Recherche en Géophysique Europe/Afrique” (GIRGEA) for

415 cooperation organisation, especially Christine Amory. JK thanks Professor Albert Kazadi  
416 from University of Kinshasa for his support, help and discussions.

## 417 **References**

418 Abarca, S.F., Corbosiero, K.L., Vollaro, D.: The World Wide Lightning Location Network  
419 and convective activity in tropical cyclones, *Mon. Weather Rev.* 139, 175–191, 2011.

420 Albrecht, R. I., Goodman, S. J., Petersen, W. A., Buechler, D. E., Bruning, E. C., Blakeslee,  
421 R. J., and Christian, H. J.: The 13 years of TRMM Lightning Imaging Sensor: from  
422 individual flash characteristics to decadal tendencies, *Proceedings of the XIV International*  
423 *Conference on Atmospheric Electricity*, 08-12 August 2011, Rio de Janeiro, Brazil, 2011.

424 Albrecht, R., Goodman, S., Buechler, D., Blakeslee, R., and Christian, H.: Where are the  
425 lightning hotspots on Earth?, *Bull. Amer. Meteor. Soc.*, 97, 2051-2068, doi:10.1175/bams-  
426 d-14-00193.1, 2016.

427 Carey, L. D., M. J. Murphy, T. L. McCormick, and N. W. S. Demetriades (2005), Lightning  
428 location relative to storm structure in a leading-line, trailing-stratiform mesoscale  
429 convective system, *J. Geophys. Res.*, 110, D03105, doi:10.1029/2003JD004371.

430 Cecil, D., Buechler, D. E., and Blakeslee, R. J.: Gridded lightning climatology from TRMM-  
431 LIS and OTD: Dataset description, *Atmos. Res.*, 135, 404-414, doi: 10.1016 /  
432 j.atmosres.2014.06.028, 2014.

433 Christian, H. J., Blakeslee, R. J., Boccippio, D. J., Boeck, W. L., Buechler, D. E., Driscoll, K.  
434 T., Goodman, S. J., Hall, J. M., Koshak, W. J., Mach, D. M., and Stewart, M. F.: Global  
435 frequency and distribution of lightning as observed from space by the Optical Transient  
436 Detector, *J. Geophys. Res.*, 108, D1, 4005, doi:10.1029/2002JD002347, 2003.

437 Dowden, R. L., Brundell, J. B., and Rodger, C. J.: VLF lightning location by time of group  
438 arrival (TOGA) at multiple sites, *J. Atmos. Solar-Terr. Phys.*, 64, 817-830, 2002.

439 Farnsworth, A., White, E., Williams, C. J. R., Black, E., and Kniveton, D. R.: Understanding  
440 the broad Scale Driving Mechanisms of Rainfall Variability over Central Africa, *Advances*  
441 *in Global Change Research*, 101, 43, Doi: 10,1007 / 978-90-481-3842-5\_5, 2011.

442 Garcia-Carreras, L., Parker, D. J., Taylor, C. M., Reeves, C. E., and Murphy, J. G.: Impact of  
443 mesoscale vegetation heterogeneities on the dynamical and thermodynamic properties of the

444 planetary boundary layer, *J. Geophys. Res.*, 115, D03102, doi:10.1029/2009JD012811,  
445 2010.

446 Jackson, B., Nicholson, S. E., and Klotter, D.: Mesoscale convective systems over western  
447 equatorial Africa and their relationship to large-scale circulation, *Monthly Weather Review*,  
448 137, 1272-1294, doi: 10.1175 / 2008MWR2525.1, 2009.

449 Koster, R. D., Dirmeyer, P. A., Guo, Z., Bonan, G., Chan, E., Cox, Peter, Gordon, C. T.,  
450 Kanae, S., Kowalczyk, E., Lawrence, D., Liu, P., Lu, C., Malyshev, S., McAvaney, B.,  
451 Mitchell, K., Mocko, D., Oki, T., Oleson, K., Pitman, A., Sud, Y. C., Taylor, C. M.,  
452 Versegny, D., Vasic, R., Xue, Y., and Yamada, T.: Regions of strong coupling between soil  
453 moisture and precipitation, *Science*, 305, 1138 doi: 10.1126/science.1100217, 2004.

454 Laing, A. G., and Fritsch, J. M.: Mesoscale convective complexes in Africa, *Mon. Weather*  
455 *Rev.*, 121, 2254-2263, 1993.

456 Laing, A. G., Carbone, R. E., Levizzani, V., and Tuttle, J. D.: The propagation and diurnal  
457 cycles of deep convection in northern tropical Africa, *Quart. J. Roy. Meteor. Soc.*, 134, 93–  
458 109, 2008.

459 Laing, A. G., Carbone, R. E., and Levizzani, V.: Cycles and propagation of deep convection  
460 over equatorial Africa, *Monthly Weather Review*, 129, 2832-2853, 2011.

461 Liu, C., and Zipser, E. J.: Global distribution of convection penetrating the tropical  
462 tropopause, *J. Geophys. Res.*, 110, D23104, doi: 10.1029 / 2005JD006063, 2005.

463 Mohr, K. I., and Thorncroft, C. D.: Intense convective systems in West Africa and their  
464 relationship to the African easterly jet, *Quart. J. Roy. Meteor. Soc.*, 132, 163–176, 2006.

465 Munoz, A. G., Daz-Lobaton, J., Chourio, X., Stock, M. J.: Seasonal prediction of lightning  
466 activity in north western Venezuela: Large-scale versus local drivers, *Atmos. Res.*, doi:  
467 10.1016/j.atmosres.2015.12.018, 2016.

468 Nguyen, H., and Duvel, J. P.: Synoptic wave perturbations and convective systems over  
469 equatorial Africa, *J. Climate*, 21, 6372-6388, 2008.

470 Rodger, C. J., Brundell, J. B., Holzworth, R. H., and Lay, E. H.: Growing Detection  
471 Efficiency of the World Wide Lightning Location Network, *Am. Inst. Phys. Conf. Proc.*,  
472 Coupling of thunderstorms and lightning discharges to near-Earth space: Proceedings of the  
473 Workshop, Corte (France), 23-27 June 2008, 1118, 15-20, DOI:10.1063/1.3137706, 2008.

474 Rodger, C. J., Brundell, J. B., Hutchins M., Holzworth, R. H.: The world wide lightning  
475 location network (WWLLN): Update of status and applications, 29th URSI General  
476 Assembly and Scientific Symposium (URSI GASS), Beijing (P. R. of China), 16-23 August  
477 2014.

478 Soula, S., F. Iacovella, O. van der Velde, J. Montanyà, M. Füllekrug, T. Farges, J. Bór, J.-F.  
479 Georgis, S. NaitAmor, and J.-M. Martin (2014), Multi-instrumental analysis of large sprite  
480 events and their producing storm in southern France, *Atmos. Res.*, 135, 415–431,  
481 doi:10.1016/j.atmosres.2012.10.004.

482 Soula, S., Kigotsi, K. J., Georgis, J. F., and Barthe, C.: Lightning climatology in the Congo  
483 Basin, *Atmospheric Research*, doi: 10.1016 / j.atmosres.2016.04.006, 2016.

484 Taylor, C. M., Gounou, A., Guichard, F., Harris, P. P., Ellis, R. J., Couvreur, F., and De  
485 Kauwe, M.: Satellite detection of soil moisture impacts on convection at the mesoscale,  
486 *Geophys. Res. Lett.*, 33, L03404, doi: 10.1029/2005GL025252, 2011.

487 Williams, E.R., Sători, G.: Lightning, thermodynamic and hydrological comparison of the two  
488 tropical continental chimneys, *J. of Atmos. and Sol.-Terr. Phys.*, 66, 1213-1231, 2004.

489 Zipser, E. J., Cecil, D. J., Liu, C., Nesbitt, S. W., and Yorty, D. P.: Where are the most intense  
490 thunderstorms on Earth, *Bull. Amer. Meteor. Soc.*, 1057-1071, doi: -87-8-1057, 2006.

491  
492  
493  
494  
495

496 **Table 1.** Flash count and flash density in both areas.

497

|          | Flash count |           | Maximum flash density<br>(fl yr <sup>-1</sup> km <sup>-2</sup> ) |      |
|----------|-------------|-----------|--|------|
|          | 2012        | 2013      | 2012   | 2013 |
| Area_max | 696,144     | 1,000,687 | 8.6  | 15.3 |
| Area_sec | 526,278     | 760,405   | 4.4  | 5.9  |
| ratio    | 1.32        | 1.32      | 1.94   | 2.59 |

498  
499  
500



501 **Table 2.** Number of days corresponding to lightning classes in the two study areas during the  
 502 2012 (366 days) and 2013 (362 days). The percentage is calculated in relation to the total  
 503 number of days during the year.

504

| Flash number   | CLASS | Number of days (%) |             |            |             |
|----------------|-------|--------------------|-------------|------------|-------------|
|                |       | 2012               |             | 2013       |             |
|                |       | Area_max           | Area_sec    | Area_max   | Area_sec    |
| 0 – 100        | CL0   | 7 (1.91)           | 59 (16.12)  | 4 (1.10)   | 43 (11.88)  |
| 101 – 1,000    | CL1   | 121 (33.06)        | 130 (35.52) | 80 (22.10) | 121 (33.43) |
| 1,001 – 2,000  | CL2   | 99 (27.05)         | 68 (18.58)  | 79 (21.82) | 58 (16.02)  |
| 2,001 – 3,000  | CL3   | 73 (19.94)         | 52 (14.21)  | 70 (19.34) | 52 (14.36)  |
| 3,001 – 4,000  | CL4   | 30 (8.20)          | 24 (6.56)   | 43 (11.88) | 29 (8.01)   |
| 4,001 – 5,000  | CL5   | 16 (4.37)          | 17 (4.64)   | 38 (10.50) | 17 (4.70)   |
| 5,001 – 6,000  | CL6   | 10 (2.73)          | 7 (1.91)    | 18 (4.97)  | 12 (3.31)   |
| 6,001 – 7,000  | CL7   | 4 (1.09)           | 4 (1.09)    | 12 (3.31)  | 11 (3.04)   |
| 7,001 – 8,000  | CL8   | 2 (0.55)           | 1 (0.27)    | 7 (1.93)   | 10 (2.76)   |
| 8,001 – 9,000  | CL9   | 4 (1.09)           | 1 (0.27)    | 2 (0.55)   | 2 (0.55)    |
| 9,001 – 10,000 | CL10  | 0 (0.00)           | 0 (0.00)    | 2 (0.55)   | 2 (0.55)    |
| > 10,000       | CL11  | 0 (0.00)           | 0 (0.00)    | 7 (1.93)   | 5 (1.38)    |
| Total          |       | 366 (100)          | 366 (100)   | 362 (100)  | 362 (100)   |

505

506

507

508

509

510

511

512

513

514

515

516

517

518  
 519  
 520  
 521  
 522  
 523  
 524  
 525  
 526  
 527  
 528  
 529  
 530  
 531  
 532  
 533  
 534  
 535  
 536  
 537  
 538  
 539  
 540  
 541  
 542

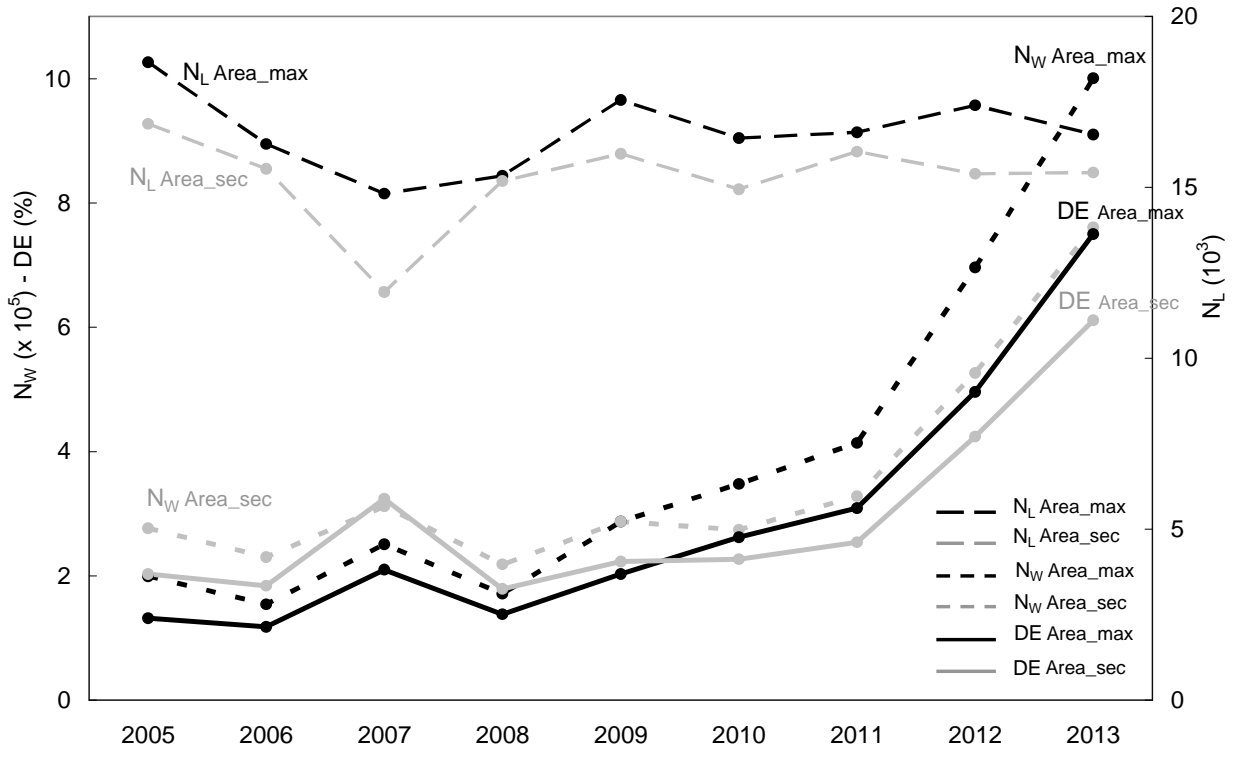
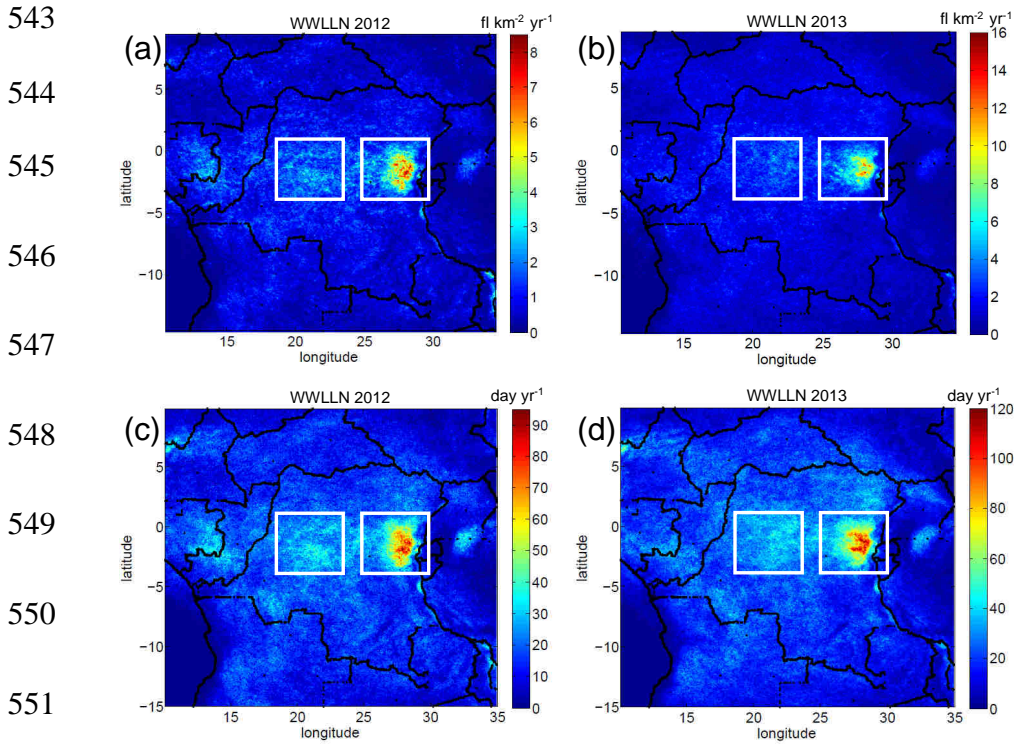


Figure 1. Annual number of flashes detected by the WWLLN ( $N_W$ ) and that detected by LIS ( $N_L$ ) for each area, and estimated detection efficiency (DE) for WWLLN data relative to LIS data, according to the methodology developed in Soula et al. (2016).



552

553 Figure 2. (a) and (b) Lightning density in  $\text{fl km}^{-2} \text{yr}^{-1}$  calculated at a resolution of  $0.05^\circ$  from  
 554 WWLLN data in the area of Congo Basin for 2012 and 2013, respectively. (c) and (d)  
 555 Number of days of the year with thunderstorm activity in the same area with a resolution of  
 556  $0.05^\circ$  for 2012 and 2013, respectively. The white frames indicate the two zones with strong  
 557 activity (left Area\_sec and right Area\_max).

558

559

560

561

562

563

564

565

566

567

568

569  
570  
571  
572  
573  
574  
575  
576  
577  
578  
579  
580  
581  
582  
583  
584  
585  
586  
587  
588  
589  
590  
591  
592  
593

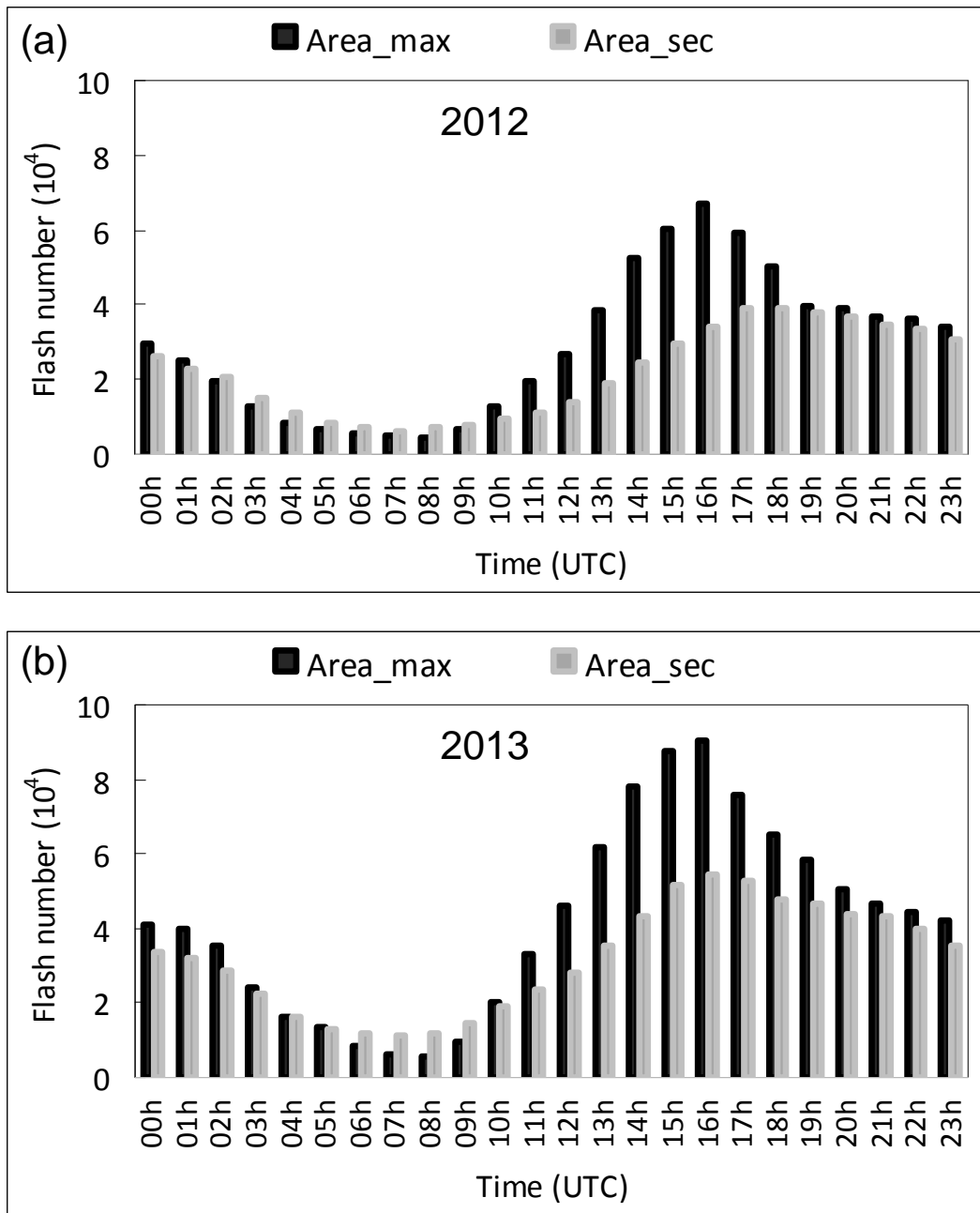


**Figure 3.** Daily evolution of the hourly lightning flash counts in Area\_max and Area\_sec for 2012 (a) and 2013 (b).

594  
595  
596  
597  
598  
599  
600  
601  
602  
603  
604  
605  
606  
607  
608  
609  
610  
611  
612  
613  
614  
615  
616  
617  
618

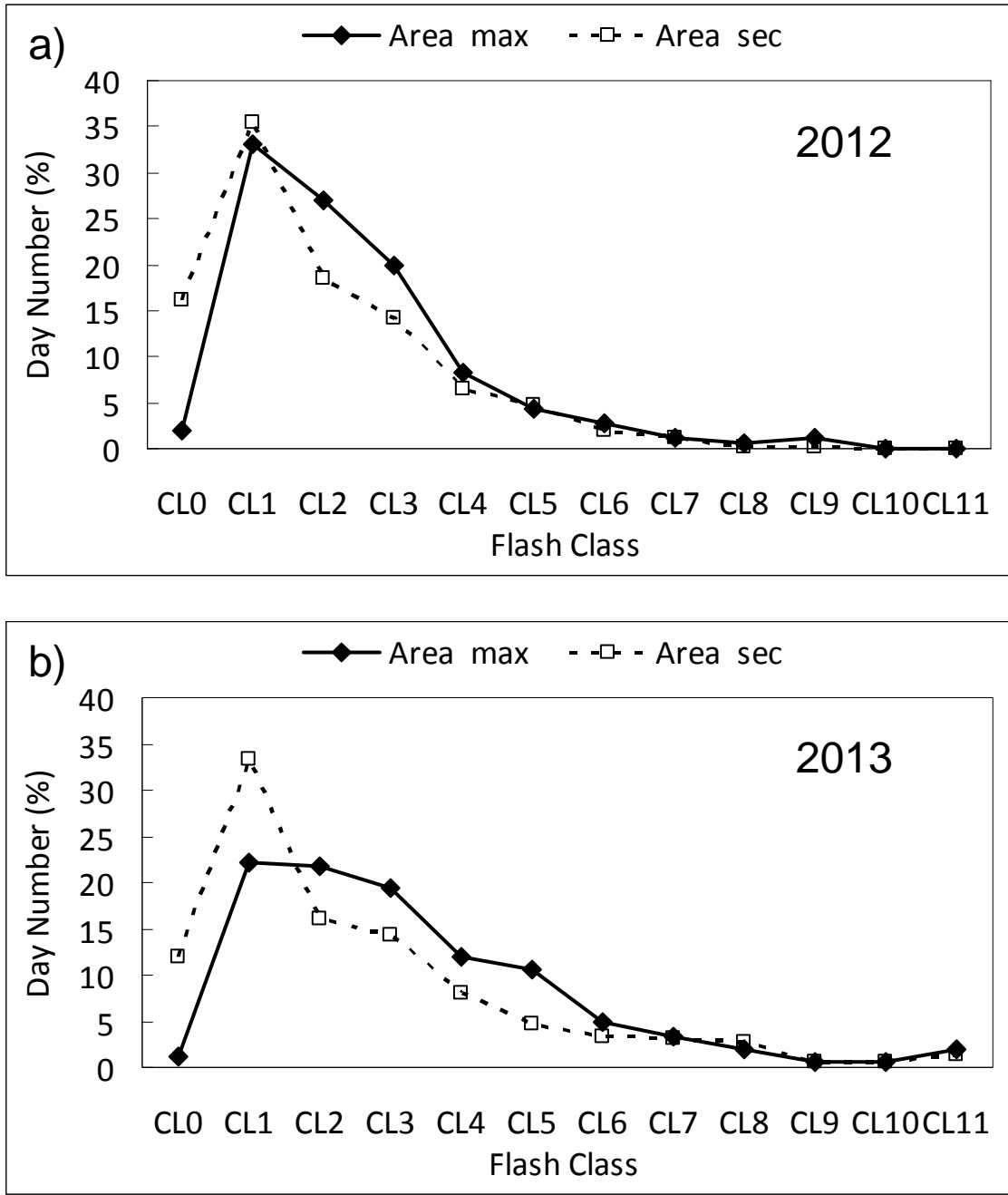


**Figure 4.** Distribution of the number of days (% of the annual number of days) versus the classes of flash number in both areas: (a) for 366 days in 2012, (b) for 362 days in 2013.

619

620

621

622

623

624

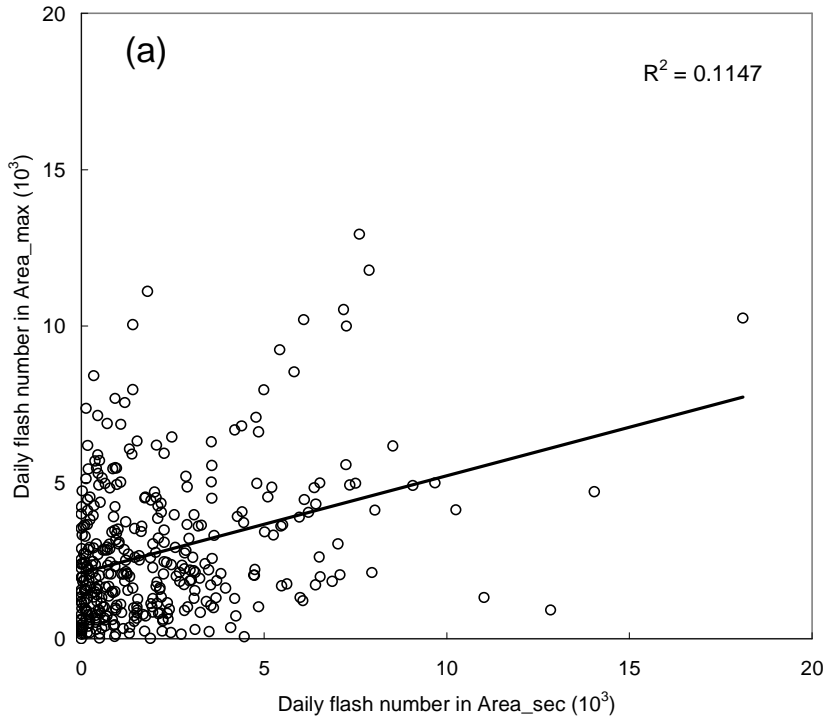
625

626

627

628

629



630

631

632

633

634

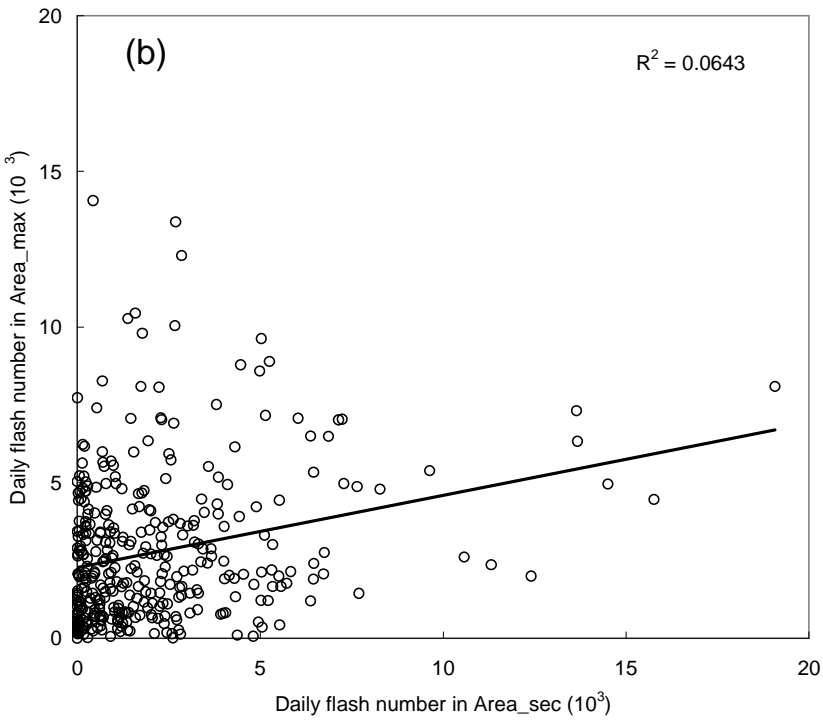
635

636

637

638

639



640

641 **Figure 5.** Diagrams of correlation between daily numbers of lightning flashes for Area\_max

642 and Area\_sec in 2013: (a) at calendar daily scale (00h00-24h00 UTC) and (b) at lightning

643 activity daily scale (06h00-06h00 UTC).

644

645

646

647

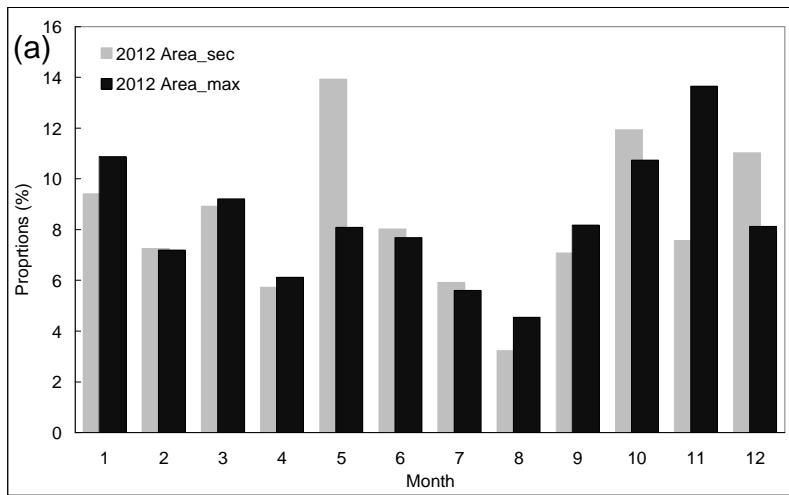
648

649

650

651

652



653

654

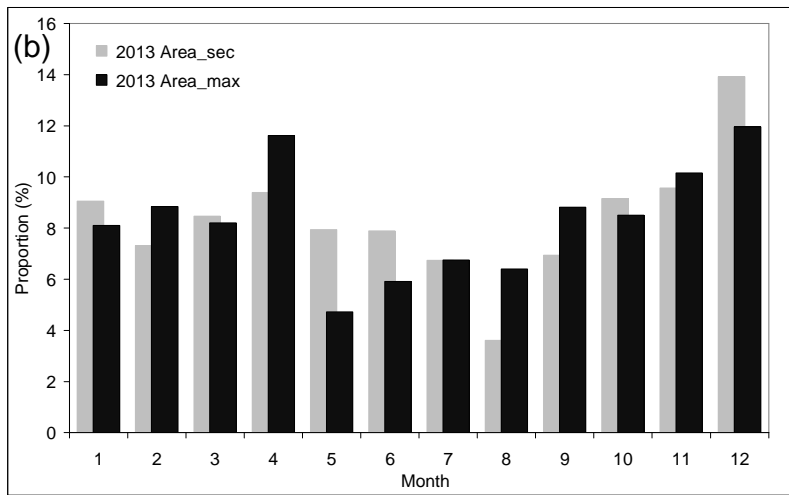
655

656

657

658

659



660

661

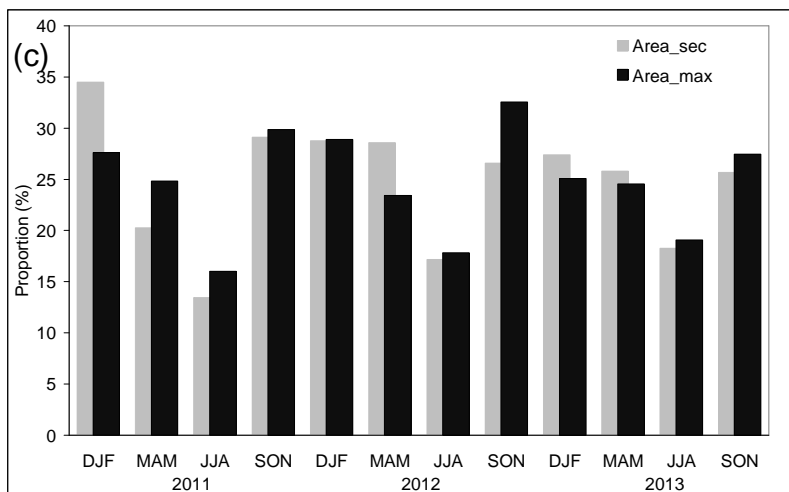
662

663

664

665

666



667 Figure 6. Proportions of flashes detected by WWLLN in Area\_max and Area\_sec: monthly  
668 (a) in 2012 and (b) 2013, and (c) seasonally in the period 2011-2013.

669

670

671

672

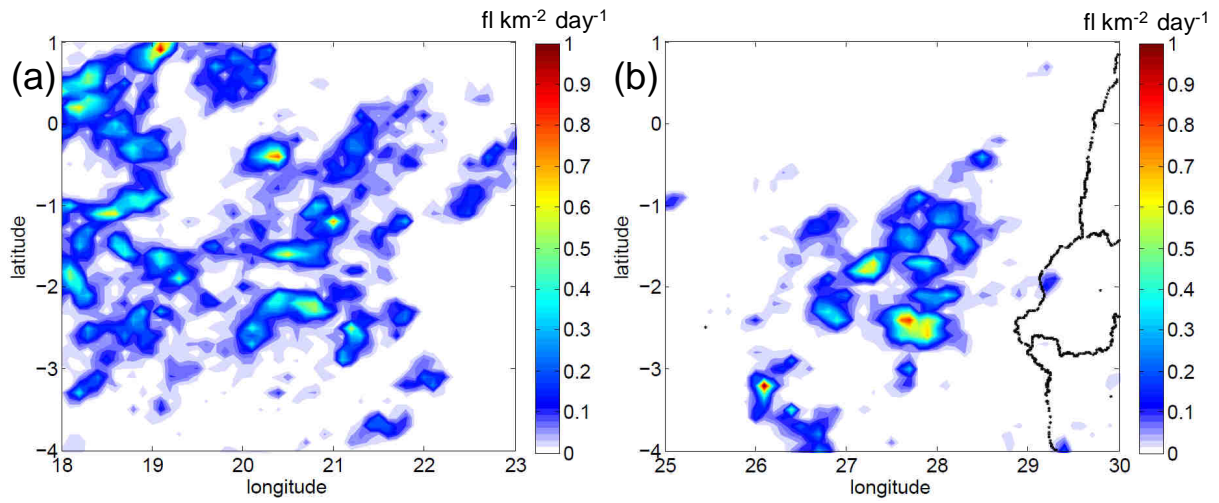
673

674

675

676

677



678 **Figure 7.** Density of lightning flashes (fl km<sup>-2</sup> day<sup>-1</sup>) detected by WWLLN on 25<sup>th</sup> of  
679 December 2013, (a) in Area\_sec and (b) in Area\_max.

680

681

682